Croatian Society for Materials Protection

*Metalurgija/Metallurgy*

**Vol. 66 No. 2 / 2027**

# Optimization and Utilization of Bai Ma Vanadium-Titanium Pellet Ore Based on Orthogonal Method

**M. Zhou [1,*], H. R. He [1], P. Hu [1], W. P. Wang [2], X. Z. Liu [1,2], W. B. Tang [1,2], L. Meng [3], J. T. Rao [1], Y. Li [2], and W. Y. Gao [4,*]**

https://doi.org/10.64486/m.66.2.7

[1] Vanadium and Titanium Resources High-Value Utilization Key Laboratory of Sichuan Province, Panzhihua, China
[2] School of Metallurgy, Northeastern University, Shenyang, China
[3] School of Geology and Mining Engineering, Xinjiang University, Urumqi, China
[4] School of Resources and Civil Engineering, Northeastern University, Shenyang, China
* Correspondence: zhoum@smm.neu.edu.cn; gaowenyuan@mail.neu.edu.cn

*Type of the Paper:* Article
*Received:* July 4, 2026
*Accepted:* August 20, 2026

**Abstract:** Under the "dual carbon" policy, efficient utilization of upgraded vanadium-titanium magnetite has become increasingly important for high-proportion pellet smelting. This study investigates the effects of preheating temperature, preheating time, roasting temperature, and roasting time on the compressive strength and microstructural evolution of fluxed Baima pellets with a basicity of 1.3 using an orthogonal experimental design. Roasting temperature had the greatest influence on compressive strength, followed by roasting time, preheating time, and preheating temperature. Range analysis predicted an optimal factor-level combination of 1000 °C/20 min/1300 °C/15 min, while the highest experimentally measured compressive strength, 2806.2 N/P, was obtained in experiment No. 7 at 1000 °C/10 min/1300 °C/15 min. With increasing roasting temperature, hematite sintering was enhanced, the liquid-phase fraction increased, porosity decreased, and hematite grains grew substantially, resulting in a denser pellet structure.

**Keywords:** vanadium-titanium magnetite; flux-type pellet; compressive strength; microstructure

## 1. Introduction

Vanadium-titanium magnetite is a composite mineral resource rich in various valuable elements such as iron, vanadium, and titanium. It is an important source of iron, vanadium, and titanium in China, with broad application prospects [1–3]. Currently, under the national 'dual carbon' policy, high-proportion pellet blast furnace smelting has become a development trend. Panzhihua Steel (Xi chang Steel and Vanadium) has built a 3-million-ton/year pellet line, reducing the cost per ton of iron by about 150 yuan. Therefore, the preparation of pellets from vanadium-titanium iron concentrate, especially fluxed pellets, represents an important approach to the low-cost smelting of vanadium-titanium magnetite. In addition, the effect of basicity on pellet quality is also significant [4–6].

The Baima mining area is one of the four vanadium-titanium mining areas currently in production in Panzhihua [7–9]. With the implementation of the new ore dressing and quality improvement process of Pan Steel Group, the TFe grade of Baima vanadium-titanium quality-improved iron concentrate has increased from 55.05 % to 57.5 %, and the $SiO_2$ content has decreased from 3.64 % to 2.50 %, with significant changes in chemical


https://doi.org/10.64486/m.66.2.7

composition and physical properties. If the upgraded Baima vanadium-titanium iron concentrate is used for pellet production, the pellet basicity should be increased to 1.3 to ensure the stability of the final slag basicity. Therefore, the roasting process parameters for preparing high-basicity flux pellets should be changed.

Regarding the impact of different roasting regimes on pellet ore, Meng et al. found that vanadium-titanium magnetite pellets need to be oxidized for a relatively long time at medium and low temperatures. Insufficient oxidation time at medium and low temperatures is the main reason for the low compressive strength of vanadium-titanium pellets [10]. Yi et al. studied the compressive strength of vanadium-titanium pellets and found that when the preheating temperature is 950 °C, the preheating time is 18 min, the firing temperature is 1300 °C, and the firing time is 10 min, the compressive strength of a single pellet can reach 2344 N [11]. The above studies indicate that different roasting regimes have a significant impact on the compressive strength of pellets made from different iron concentrates, and the optimal roasting regime for different pellets is not the same [12–13].

On this basis, this study uses the upgraded Baima vanadium-titanium iron concentrate as the raw material and applies an orthogonal experimental design to investigate the effects of different roasting regimes on the compressive strength, phase composition, and microstructure of fluxed pellets with a basicity of 1.3.

This paper systematically investigates the roasting process of high-basicity pellets prepared from upgraded Baima vanadium-titanium iron concentrate, identifies the key factors affecting pellet strength, and provides new data to support the efficient utilization of similar resources.

## 2. Materials and Methods

This study focuses on BM ore from the Panzhihua Baima mining area, a newly produced vanadium-titanium iron concentrate obtained through optimized beneficiation processes. Compared with the original Baima iron concentrate, the upgraded concentrate has an improved chemical composition, as shown in Table 1. As indicated in Table 1, the upgraded Baima vanadium-titanium iron concentrate has a TFe content of 57.50 %, representing an increase of 2.45 percentage points compared with the original Baima concentrate (55.05 %). The $SiO_2$ content decreased from 3.64 % to 2.50 %, while the MgO and $Al_2O_3$ contents decreased by 0.50 and 0.20 percentage points, respectively.

The limestone powder used in the experiment was sourced from the site, and its chemical composition is shown in Table 1, with a CaO content of 52.50 %. The main chemical composition and physical and chemical properties of the bentonite are shown in Table 1 and Table 2, with a montmorillonite mass fraction of 68.3 %, a water absorption rate of 237.5 %, a plasticity index of 62.0 %, a methylene blue adsorption capacity of 34.0 g/(100 g), and a swelling volume of 42 mL/g.

**Table 1**. Chemical compositions of raw materials /mas. %

| Items | TFe | CaO | $SiO_2$ | $TiO_2$ | $V_2O_5$ | MgO | $Al_2O_3$ | FeO |
|---|---|---|---|---|---|---|---|---|
| BM ore | 57.50 | 0.40 | 2.50 | 10.3 | 0.72 | 3.00 | 3.30 | 32.00 |
| Limestone | — | 52.50 | 2.50 | — | — | 0.50 | 1.00 | — |
| Bentonite | — | 12.00 | 61.00 | — | — | 2.00 | 9.00 | — |

**Table 2**. Physicochemical properties of bentonite

| Colloid index wt % | Expansion volume mL/g | Water absorption content 2 h/wt % | Methylene blue absorbed g/(100 g) | Montmorillonite content wt % |
|---|---|---|---|---|
| 62.0 | 42.0 | 237.5 | 34.0 | 68.3 |

Figures 1 and 2 show the SEM-EDS and XRD results of the Baima vanadium-titanium upgraded iron concentrate, respectively. As shown in Figures 1 and 2, the particles of the Baima vanadium-titanium upgraded iron concentrate are relatively fine, mainly in the form of flakes and plates, with some fine gangue particles and a small amount of plate-like iron olivine particles distributed between the titanomagnetite grains. The main


https://doi.org/10.64486/m.66.2.7

mineral phases in the Baima vanadium-titanium upgraded concentrate are titanomagnetite ($Fe_{2.75}Ti_{0.25}O_4$) and magnetite ($Fe_3O_4$), with a small amount of ilmenite ($FeTiO_3$), and vanadium occurs in magnetite in the form of isomorphous substitution [14–16].

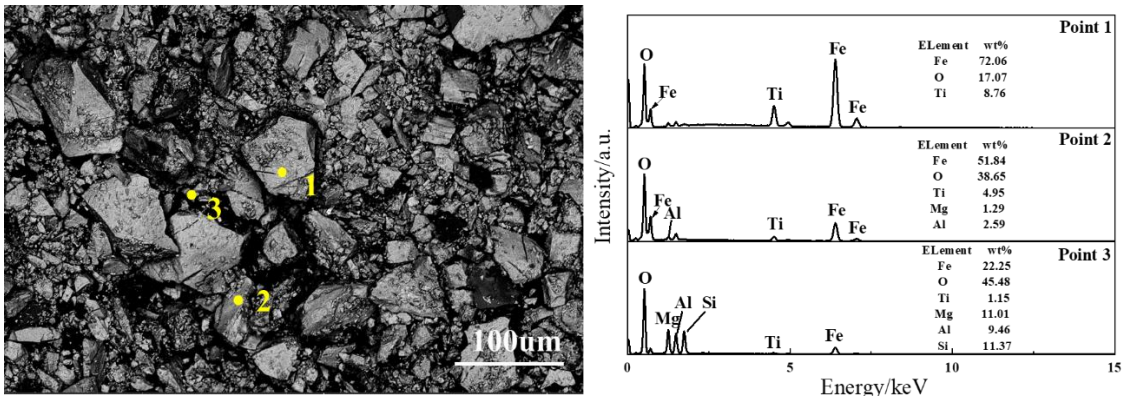


**Figure 1**. SEM micrographs and EDS analysis results of the BM ore

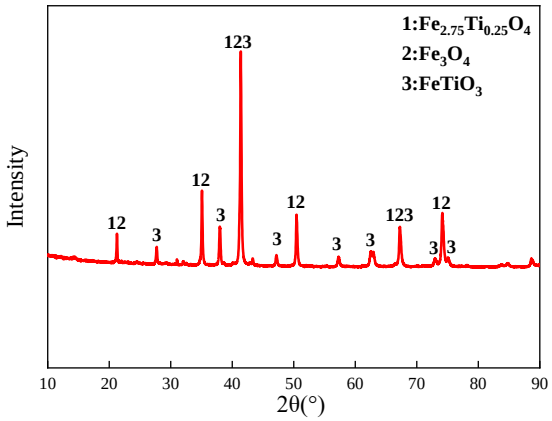


**Figure 2**. XRD analysis of the BM ore

The particle size distribution of the raw materials was analyzed using a BT-9300ST laser particle size analyzer, with a testing range of (0–1000) μm and an obscuration set at (14–16) %. The results are shown in Table 3 and Figure 3.

**Table 3**. Particle size distribution of raw materials / %

| Items | Size | | | |
|---|---|---|---|---|
| | ＜0.046 mm | (0.046, 0.074] mm | (0.074, 0.15] mm | ＞0.15 mm |
| BM ore | 88.75 | 7.72 | 3.26 | 0.27 |
| Limestone | 93.20 | 4.96 | 1.84 | — |
| Bentonite | 97.94 | 1.95 | 0.11 | — |


https://doi.org/10.64486/m.66.2.7

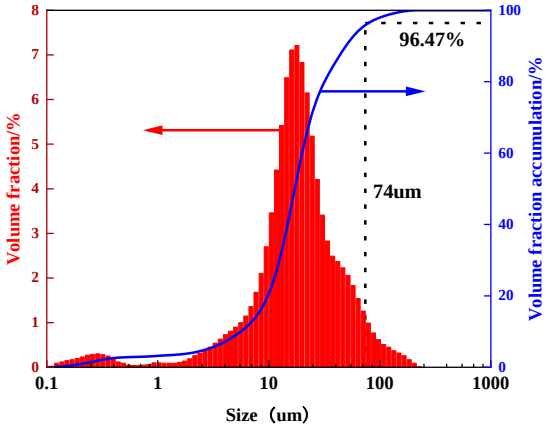


**Figure 3**. BM ore particle size distribution

As shown in Table 3 and Figure 3, the proportions of the three raw materials with a particle size <0.046 mm are 88.75 %, 93.2 %, and 97.94 %, respectively; the proportions with a particle size <200 mesh (0.074 mm) are 96.47 %, 98.16 %, and 99.89 %, respectively. The particle sizes are relatively fine, all exceeding 80 %, which meets requirements for raw material pelletizing.

Figure 4 shows the experimental procedure. BM ore, limestone powder, and bentonite were mixed in a V-20 mixer at a ratio of 90:8:2 (the theoretical binary basicity at 1.3); the material mixed for 15 min was fed into a disc pelletizer for pelletizing. The pelletizing parameters are: disc 1000 mm, inclination angle 45°, rotational speed adjusted to 12 r/min, pelletizing time (25±2) min, and pellet moisture (8.0±0.5) %. The size of the green pellets was controlled at (10–12.5) mm. After pelletizing, the green pellets were placed in a drying oven at 105 °C for drying. The dried green pellets underwent oxidative roasting treatment. Subsequently, the roasted pellets were subjected to a compressive strength test.

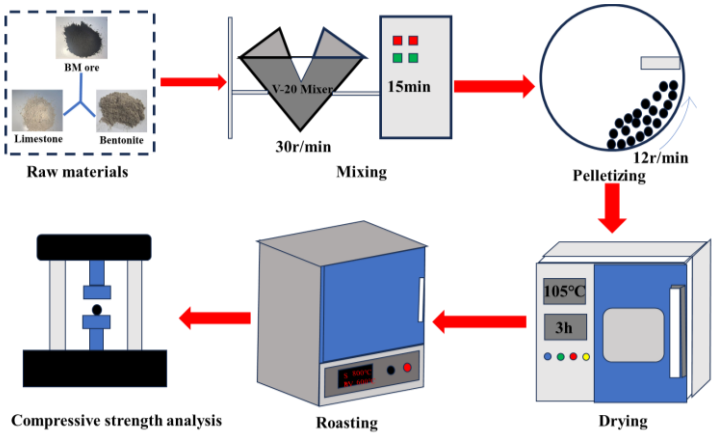


**Figure 4**. Experimental procedure

Figure 5 shows the temperature curve during the oxidative roasting of pellets. Table 4 shows the roasting orthogonal experimental design with 4 factors and 3 levels.


https://doi.org/10.64486/m.66.2.7

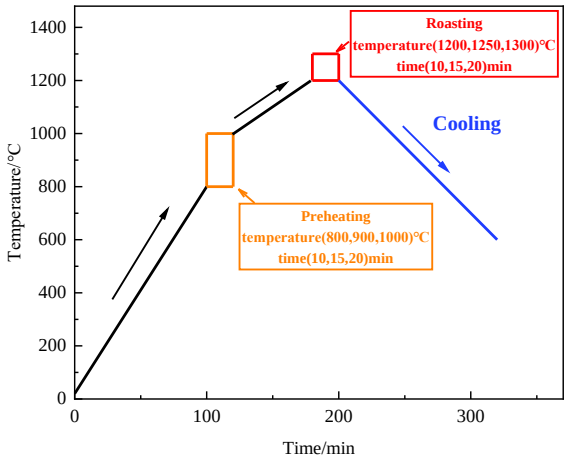


**Figure 5**. Temperature curve during the oxidative roasting of pellets

**Table 4**. BM Ore Oxidation Roasting Experimental Plan

| Items | Preheating Temperature / °C | Preheating Time / min | Roasting temperature / °C | Roasting Time / min |
|---|---|---|---|---|
| NO.1 | 800 | 10 | 1200 | 10 |
| NO.2 | 800 | 15 | 1250 | 15 |
| NO.3 | 800 | 20 | 1300 | 20 |
| NO.4 | 900 | 10 | 1250 | 20 |
| NO.5 | 900 | 15 | 1200 | 10 |
| NO.6 | 900 | 20 | 1300 | 15 |
| NO.7 | 1000 | 10 | 1300 | 15 |
| NO.8 | 1000 | 15 | 1200 | 20 |
| NO.9 | 1000 | 20 | 1250 | 10 |

## 3. Results and discussion

### 3.1 Orthogonal results of pellet compressive strength

The compressive strength of the pellets was tested using a compressive strength tester. Table 5 and Figure 6 present the orthogonal results of the compressive strength of pellet ore roasting experiments.

**Table 5**. Orthogonal results of pellet compressive strength

| Items | I | II | III | IV | CCS/N·P$^{-1}$ |
|---|---|---|---|---|---|
| | Preheating temperature / °C | Preheating time min | Roasting temperature / °C | Roasting time min | |
| NO.1 | 800 | 10 | 1200 | 10 | 1492.8 |
| NO.2 | 800 | 15 | 1250 | 15 | 2218.5 |
| NO.3 | 800 | 20 | 1300 | 20 | 2411.2 |
| NO.4 | 900 | 10 | 1250 | 20 | 2114.5 |
| NO.5 | 900 | 15 | 1200 | 10 | 1528.6 |
| NO.6 | 900 | 20 | 1300 | 15 | 2552.7 |
| NO.7 | 1000 | 10 | 1300 | 15 | 2806.2 |
| NO.8 | 1000 | 15 | 1200 | 20 | 1592.5 |
| NO.9 | 1000 | 20 | 1250 | 10 | 2149.6 |
| K1 | 6122.5 | 6413.5 | 4613.9 | 5171 | |
| K2 | 6195.8 | 5339.6 | 6482.6 | 7577.4 | |


https://doi.org/10.64486/m.66.2.7

| Items | I<br>Preheating temperature / °C | II<br>Preheating time min | III<br>Roasting temperature / °C | IV<br>Roasting time min | CCS/N·P$^{-1}$ |
|---|---|---|---|---|---|
| K3 | 6548.3 | 7113.5 | 7770.1 | 6118.2 | |
| k1 | 2040.8 | 2137.8 | 1538.0 | 1723.7 | |
| k2 | 2065.2 | 1779.9 | 2160.9 | 2525.8 | |
| k3 | 2182.7 | 2371.2 | 2590.0 | 2039.4 | |
| R | 141.9 | 591.3 | 1052.1 | 802.1 | |

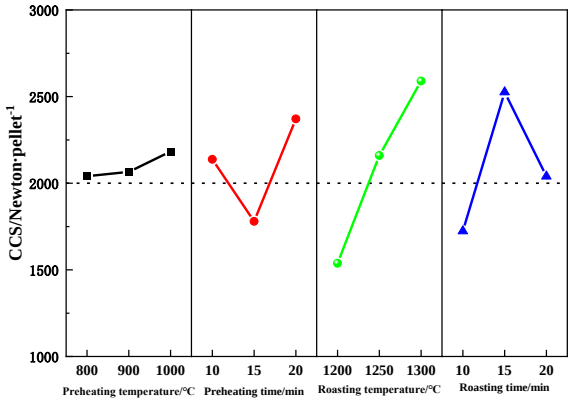


**Figure 6**. Orthogonal results of pellet compressive strength

As shown in Table 5 and Figure 6, R(I) = 141.9, R(II) = 591.3, R(III) = 1052.1, R(IV) = 802.1, and R(III) > R(IV) > R(II) > R(I). Therefore, according to the range analysis, the factors affecting the compressive strength of roasted Baima vanadium-titanium pellets in order are: roasting temperature > roasting time > preheating time > preheating temperature. According to the range analysis, the predicted optimal factor-level combination is I3II3III3IV2, corresponding to a preheating temperature of 1000 °C, a preheating time of 20 min, a roasting temperature of 1300 °C, and a roasting time of 15 min. This combination was not included among the nine experimental runs and therefore requires experimental verification.

The highest experimentally measured compressive strength, 2806.2 N/P, was obtained in experiment No. 7 at a preheating temperature of 1000 °C, a preheating time of 10 min, a roasting temperature of 1300 °C, and a roasting time of 15 min. Based on its lower thermal requirements, a combination of a preheating temperature of 800 °C, a preheating time of 10 min, a roasting temperature of 1250 °C, and a roasting time of 15 min is proposed as a candidate energy-saving regime. Since this combination was not included among the experimental runs, its compressive strength and actual energy consumption must be experimentally verified.

### *3.2 Pellet phase results*

Figure 7 shows the XRD analysis results of three typical roasting regimes. The phases identified in the Baima pellets are $Fe_9TiO_{15}$, hematite ($Fe_2O_3$), pseudobrookite ($Fe_2TiO_5$), and ilmenite ($FeTiO_3$). Analysis of the X-ray diffraction patterns reveals that the intensity of the $Fe_2TiO_5$ peak decreases from No. 7 to No. 1, while the $Fe_9TiO_{15}$ peak shows the opposite trend.


https://doi.org/10.64486/m.66.2.7

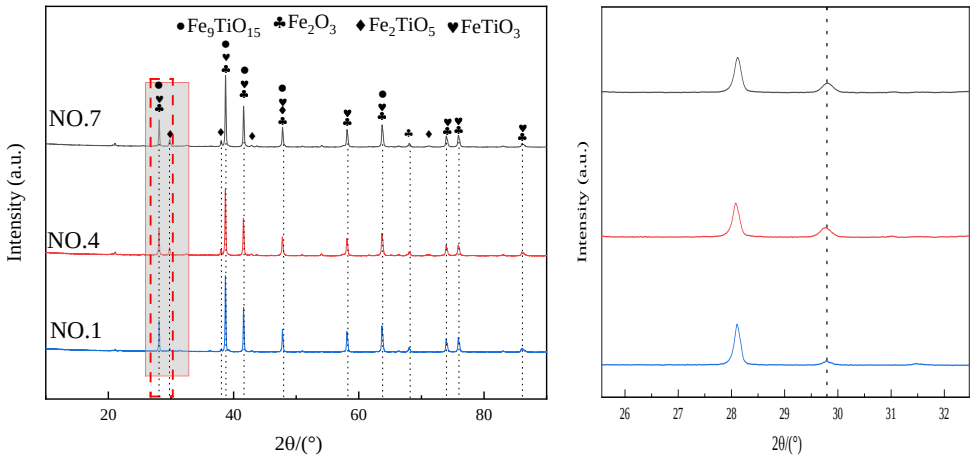


**Figure 7**. XRD analysis results of BM pellets

The observed differences in the XRD patterns among the three roasting regimes suggest changes in phase composition associated with the different processing conditions. In particular, the changes in the $Fe_2TiO_5$ and $Fe_9TiO_{15}$ peak intensities are consistent with increased pseudobrookite formation under the higher-temperature roasting regimes. These phase changes may contribute to the observed differences in pellet compressive strength.

*3.3 Microstructure of pellets*

The internal phases of the nine pellet groups were observed using a mineralogical microscope. Five representative pellets with good sphericity and similar morphology were selected from each group for photomicrography. For each pellet, 64 photomicrographs arranged in an 8 × 8 grid were acquired and stitched to reconstruct the pellet cross-section.

A representative area located at approximately half the pellet radius, corresponding to the transition between the outer and inner regions, was selected for analysis. Grain size was determined using the linear intercept method, with approximately 500 grains measured. Porosity and phase proportions were determined using Image-Pro software and grayscale threshold segmentation, with grayscale values of 0–70 assigned to pores, 70–140 to the liquid phase, and 140–255 to the hematite phase. Figure 8 shows the cross-sections of Groups No. 1, No. 4, and No. 7, while Figure 9 presents the microstructures of Groups No. 1–9.

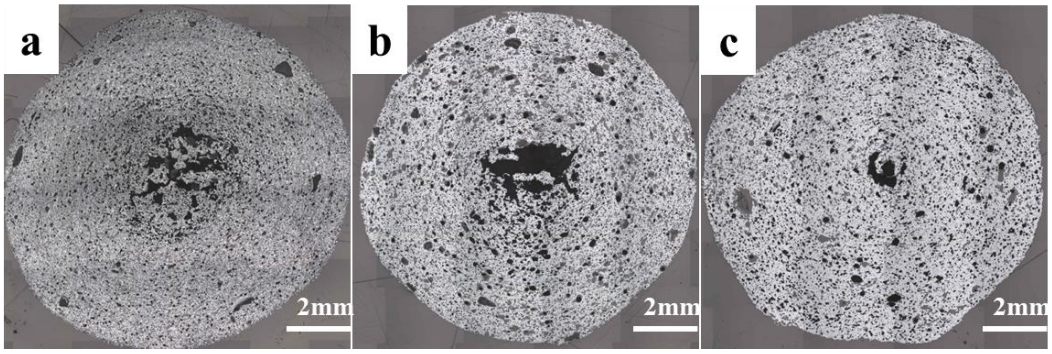


**Figure 8**. Cross-section of the BM pellets

As shown in Figure 8, Groups No. 1, No. 4, and No. 7 were obtained under different preheating and roasting conditions. Group No. 1 contains more black regions, indicating a higher amount of unoxidized magnetite, together with smaller grains, weaker crystal intergrowth, and a greater number of internal pores,


https://doi.org/10.64486/m.66.2.7

resulting in a lower compressive strength of 1492.8 N/P. In contrast, Group No. 7 exhibits better-developed grains, stronger hematite intergrowth, and a more uniform distribution of internal voids. These microstructural characteristics may contribute to its higher compressive strength of 2806.2 N/P.

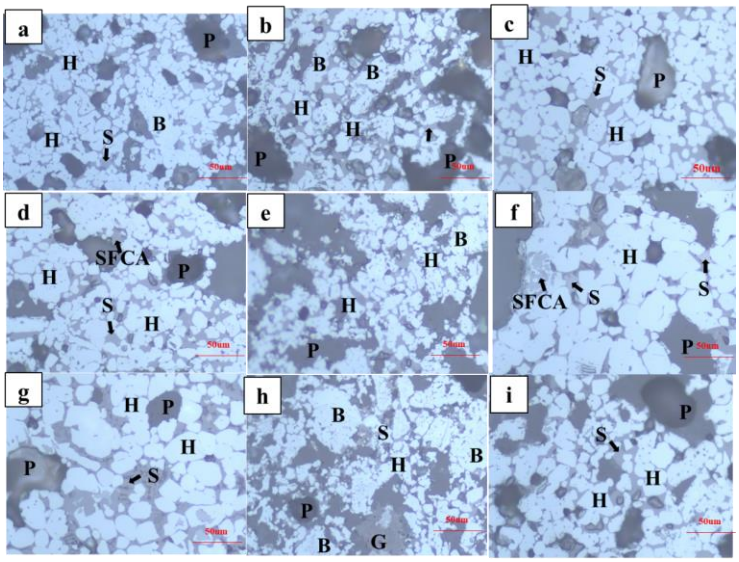


H—Hematite，B—pseudobrookite，S—slag，P—hole，SFCA—Calcium ferrite

**Figure 9**. Microstructure of BM pellets

As shown in Figure 9, the Baima vanadium-titanium pellets are mainly composed of hematite, titanomagnetite, and pseudobrookite, with a small amount of slag and gangue phases [17–19]. In Groups (a), (e), and (h), corresponding to roasting at 1200 °C, the recrystallized hematite grains are relatively small, approximately 10 μm, and the degree of interconnection between grains is limited. In Groups (c), (f), and (g), obtained under higher-temperature roasting conditions, the hematite grains are larger and more strongly interconnected, with many grains exceeding 50 μm. These microstructural differences are associated with a denser and more stable pellet structure and may contribute to the observed differences in compressive strength.

Quantitative image analysis of the pellet microstructure was performed using Image-Pro software, and Figure 10 shows the phase proportions in the nine pellet groups.

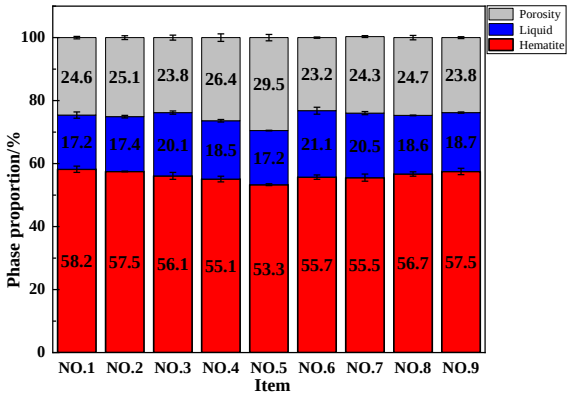


**Figure 10.** Phase proportions under different roasting regimes

As shown in Figure 10, Group No. 5 exhibits the highest porosity, 29.5 %, whereas Group No. 7 shows one of the lowest porosity values, approximately 24 %. Group No. 7 also exhibits a liquid-phase fraction above 20 %. These results indicate that the different roasting regimes are associated with changes in porosity and phase


https://doi.org/10.64486/m.66.2.7

proportions. The lower porosity and higher liquid-phase fraction observed in Group No. 7 are consistent with a denser microstructure and may contribute to its higher compressive strength.

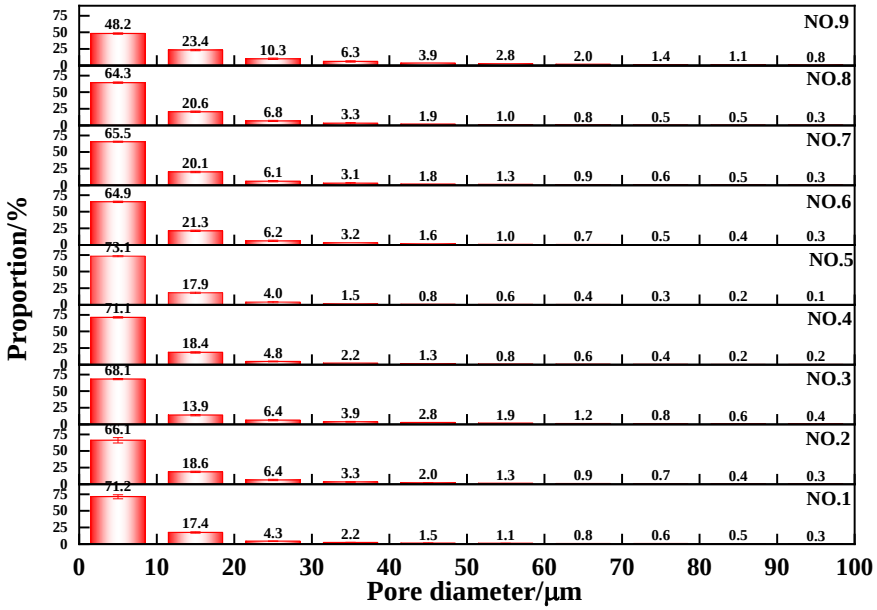


**Figure 11.** Pore-size distribution of the pellet groups

As shown in Figure 11, small pores with diameters below 20 μm account for more than 70 % of the pore population in all pellet groups. Group No. 9 exhibits the lowest proportion of small pores, 71.55 %, whereas Group No. 5 shows the highest proportion, 91.00 %. The differences in pore-size distribution among the pellet groups reflect the combined effects of the different roasting regimes. Variations in pore size and pore population may contribute to the observed differences in pellet compressive strength.

## 4. Conclusions

This study systematically investigated the effects of roasting regimes on the compressive strength and microstructure of high-basicity pellets prepared from upgraded Baima vanadium-titanium iron concentrate using an orthogonal experimental design. The factors affecting pellet compressive strength were ranked in the following order: roasting temperature > roasting time > preheating time > preheating temperature. Higher-temperature roasting regimes were associated with enhanced hematite recrystallization and grain growth, with grain sizes increasing from approximately 10 μm to more than 50 μm, together with lower porosity and a denser pellet structure. These microstructural changes may contribute to the observed increase in pellet compressive strength.

Range analysis predicted a factor-level combination of 1000 °C preheating temperature, 20 min preheating time, 1300 °C roasting temperature, and 15 min roasting time as potentially favorable for achieving high pellet strength. The highest experimentally measured compressive strength, 2806.2 N/P, was obtained in experiment No. 7 at a preheating temperature of 1000 °C, a preheating time of 10 min, a roasting temperature of 1300 °C, and a roasting time of 15 min. Based on its lower thermal requirements, a combination of 800 °C preheating temperature, 10 min preheating time, 1250 °C roasting temperature, and 15 min roasting time is proposed as a candidate energy-saving regime. Since neither the predicted optimal combination nor the proposed energy-saving combination was included among the experimental runs, confirmation experiments are required before either regime can be recommended for industrial application.


https://doi.org/10.64486/m.66.2.7

## Acknowledgments

The authors thank the National Natural Science Foundation of China (52074081, 51604065); the Key and Technology Research Project of the Department of Education of Liaoning Province (JYTZD2023048); and the Open Fund Project of the State Key Laboratory of Utilization of Vanadium and Titanium Resources (2023P4FZG06A) for supporting this research.

## References

[1] X. Zhou, X. L. Han, L. Liu, et al., "Analysis of mineralogical structure and metallurgical properties of different types of vanadium titanium pellets," *Sintering and Pelletizing*, Vol. 44, no. 4, pp. 31–35, 2019. (in Chinese). https://doi.org/10.13403/j.sjqt.2019.04.057

[2] S. T. Yang, M. Zhou, T. Jiang, et al., "Effect of CaO/SiO2 ratio on melting property and strength of sinter with vanadium-titanium iron ore addition," *Metalurgija*, Vol. 55, no. 4, pp. 585–588, 2016. https://hrcak.srce.hr/157372

[3] M. Zhou, T. Jiang, S. T. Yang, et al., "Optimization utilization of vanadium-titanium iron ore in sintering based on orthogonal method," *Metalurgija*, Vol. 55, no. 4, pp. 581–584, 2016. https://hrcak.srce.hr/en/157371

[4] W. X. Liu, H. Xiao, Z Y Hua, et al., "Effect of roasting regime on strength and metallurgical properties of fluxed pellets," *Hebei Metallurgy*, Vol. 5. no. 5. pp. 7–12,2023. https://doi.org/10.13630/j.cnki.13-1172.2023.0502

[5] H. Yu, X. F. Shi, G. Q. Yang, et al., "Process optimization for preparation of fluxed pellets from vanadium-titanium magnetite," *Journal of North China University of Science and Technology (Natural Science Edition)*, Vol. 46, no. 1, pp. 36–43, 2024. (in Chinese). https://doi.org/10.3969/j.issn.2095-2716.2024.01.005

[6] J. T. Ju, Q. D. Li, X. D. Xing, et al., "Investigations on Compressive Strength and Microstructure of High-Basicity Iron Ore Pellets," *JOM*, Vol. 75, no. 7, pp. 2525–2534, 2023. https://doi.org/10.1007/s11837-023-05747-0

[7] F. L. Chen, X. J. Yang, X. Y. Cai, et al., "Research on iron selection test of ultra-low grade vanadium-titanium magnetite of Baima Huichang type in Panxi region," *Multipurpose Utilization of Mineral Resources*, Vol. 6, pp. 26–30,2020. (in Chinese). https://doi.org/10.3969/j.issn.1000-6532.2020.06.005

[8] S. Li, F L. Chen, X. Y. Cai, et al., "Experimental study on quality improvement and impurity reduction of a vanadium-titanium iron concentrate in Panxi," *Iron Steel Vanadium Titanium*, Vol.44, no.5, pp. 105–111. 2023. (in Chinese). https://doi.org/10.7513/j.issn.1004-7638.2023.05.016

[9] Z. X. Liu, "Research and industrial practice on quality improvement and impurity reduction of Baima vanadium-titanium magnetite," *Iron Steel Vanadium Titanium*, Vol. 43, no.3, pp. 104–110. 2022. (in Chinese). https://doi.org/10.7513/j.issn.1004-7638.2022.03.017

[10] F. Y. Meng and B. F. Huang, "Research on strengthening consolidation performance of oxidized pellets of vanadium titanium magnetite," *Sintering and Pelletizing*, Vol. 45, no. 5, pp. 49–53, 2020. (in Chinese). https://doi.org/10.13403/j.sjqt.2020.05.069

[11] Y. H. Yi, G. H. Li, P. X. Cao, et al., "Effect of humic acid binder on oxidation roasting of vanadium-titanium magnetite pellets via straight-grate process," *Crystals*, Vol. 11, no. 11, Article 1283, 2021, https://doi.org/10.3390/cryst11111283

[12] T. Han, S. X. Xiao, G. J. Cheng, et al., "Preparation experiment of oxidized pellets from Liaoxi vanadium-titanium magnetite," *Multipurpose Utilization of Mineral Resources*, Vol. 6, no. 3, pp. 7–13, 2023. (in Chinese). https://doi.org/10.3969/j.issn.1000-6532.2023.03.002

[13] G. W. Zhou, W. Lv, F. R. Chen, et al., "Optimization of preparation process of high-strength pellets from Panzhihua ilmenite concentrate," *Journal of Iron and Steel Research International*, Vol. 30. pp. 2391–2402, 2023. https://doi.org/10.1007/s42243-023-00981-x

[14] L. T. Yu, X. R. Xiang, J. T. Ju, et al., "Study on oxidizing roasting behavior of pellets produced with a certain vanadium-titanium magnetite, Hami, Xinjiang," *Sintering and Pelletizing*, Vol. 50, no. 6, pp. 47–55, 2025. (in Chinese). https://doi.org/10.13403/j.sjqt.2025.06.095

[15] X. L. Chen, Y. S. Huang, X. H. Fan, et al., "Oxidation roasting behavior and concretion properties of vanadium-titanium magnetite pellet," *Journal of Central South University (Science and Technology)*, Vol. 47, no. 2, pp. 359–366, 2016. (in Chinese).

[16] R. Q. Zeng, N. Wang, and W. Li, "Non-isothermal oxidation induration mechanism of vanadium titanomagnetite pellets," *Advanced Powder Technology*, Vol. 34, no. 5, Article 104012, 2023. https://doi.org/10.1016/j.apt.2023.104012

[17] J. Tang, M. S. Chu, C. Feng, et al., "Phases Transition and Consolidation Mechanism of High Chromium Vanadium-Titanium Magnetite Pellet by Oxidation Process," *High Temperature Materials and Processes*, Vol. 35, no. 7, pp. 729–738, 2016. https://doi.org/10.1515/htmp-2015-0067

[18] H. Zhang, K. K. Bai, W. G. Liu, et al., "Effect of Magnetite Concentrate Particle Size on Pellet Oxidation Roasting Process and Compressive Strength," *ISIJ International*, Vol. 62, no. 9, pp. 1792–1801, 2022. https://doi.org/10.2355/isijinternational.ISIJINT-2022-121

[19] W. Lv, G. W. Zhou, F. R. Chen, et al., "A Novel Process for Preparing High-Strength Pellets of Ilmenite Concentrate," *Journal of Sustainable Metallurgy*, Vol. 8, pp. 551–565, 2022. https://doi.org/10.1007/s40831-022-00508-w